PCCP

Accepted Manuscript

This is an *Accepted Manuscript*, which has been through the Royal Society of Chemistry peer review process and has been accepted for publication.

Accepted Manuscripts are published online shortly after acceptance, before technical editing, formatting and proof reading. Using this free service, authors can make their results available to the community, in citable form, before we publish the edited article. We will replace this *Accepted Manuscript* with the edited and formatted *Advance Article* as soon as it is available.

You can find more information about *Accepted Manuscripts* in the Information for Authors.

Please note that technical editing may introduce minor changes to the text and/or graphics, which may alter content. The journal's standard Terms & Conditions and the Ethical guidelines still apply. In no event shall the Royal Society of Chemistry be held responsible for any errors or omissions in this *Accepted Manuscript* or any consequences arising from the use of any information it contains.

ROYAL SOCIETY OF CHEMISTRY

www.rsc.org/pccp

Synthesis of Z-scheme g-C_3N_4–Ti^{3+}/TiO_2 material: an efficient visible light photoelectrocatalyst for degradation of phenol

Wenjuan Liao[a], Muthu Murugananthan[b], Yanrong Zhang[a*]

[a] *Environmental Science Research Institute, Huazhong University of Science and Technology, Wuhan 430074, P.R. China*

[b] *Department of Chemistry, PSG College of Technology, Peelamedu, Coimbatore 641 004, India*

Abstract

In this study, a photocatalytic material g-C_3N_4–Ti^{3+}/TiO_2 nanotube arrays, was prepared by a facile and viable approach involving a heat treatment followed by an electrochemical reduction step, and it was characterized by using instrumental techniques such as X-ray diffraction pattern, Fourier transform-infrared spectroscopy, X-ray photoelectron spectroscopy, scanning electron microscopy and UV–vis diffuse reflectance spectra. The photocatalytic efficiency of the as-prepared samples towards treating aqueous solution contaminated with phenol was systematically evaluated by photoelectrocatalytic method and found to be highly dependent on content of the g-C_3N_4. At the optimal content of g-C_3N_4, the apparent photocurrent density of g-C_3N_4–Ti^{3+}/TiO_2 was four times higher than that of the pristine TiO_2 under visible-light illumination. The enhanced photoelectrocatalytic behavior observed for g-C_3N_4–Ti^{3+}/TiO_2, was ascribed to a cumulative impact of both g-C_3N_4 and Ti^{3+} which widen the photo responsive behavior of the material into visible region and facilitate the effective charge separation of photo-induced charge carriers.

---

[*] Corresponding author: Tel: +86 27 87793001; Fax: +86 27 87793001.

Email address: yanrong_zhang@ hust.edu.cn.

Physical Chemistry Chemical Physics Accepted Manuscript

Physical Chemistry Chemical Physics Accepted Manuscript

1. Introduction

As known, photocatalytic materials are being well employed for the applications of production of energy/fuel and preservation of cleaner environment such as wastewater treatment, hydrogen generation by water splitting method and conversion of CO_2 into hydrocarbon fuel.[1-3] Nevertheless, the most widely used TiO_2 photocatalyst, is often yielding poor performance and ineffective due to two major problems that include wide bandgap (3.0-3.2 eV) and low quantum efficiency.[4, 5] To overcome these problems and improve the efficiency of the photocatalytic material, the absorption wavelength can be widened and secondly the effective charge separation can be made between photoexcited electron-hole pair.

Much attention has been paid to a possibility of narrowing the bandgap of TiO_2, thereby enhancing the visible light absorption behavior of the material. The general strategies for modifying TiO_2 include energy band modulation by doping with metal elements (Fe and Cu) [6, 7] and non-metal elements (N and S).[8, 9] It is believed that bulk doping or matrix substitution could very well introduce interior electron energy states between the band gap thus the light response region of the material can be extended to the visible range. In addition, in the case of metal ion implantation, replacement of Ti^{4+} by Ti^{3+} in the lattice by doping could yield donor states below the conduction band, that can result in improved light absorption and charge transport behavior similar to a n-type doping of the material.[10, 11]

A study on synthesis of a composite of TiO_2 with other semiconductors to form heterojunction structured material was demonstrated to be useful for improving the photocatalytic activity of TiO_2-based materials, owing to effective separation of electron-hole charge pairs and decreasing the rate of their recombination as well. [12] The transfer of the photoexcited carriers between the heterojunction is possible either

Physical Chemistry Chemical Physics Accepted Manuscript

by band to band or Z-scheme principle transfers. The former transfer is between valence band (VB) and conduction band (CB), [13-16] in which photoexcited holes get upflow to the higher level of VB and photoexcited electrons conversely get downflow to the lower level of CB, which limits the photo-oxidation and photo-reduction ability of the composite material to the respective lower level of the pristine catalyst. Whereas in Z-scheme principle transfer, photoexcited electrons of conduction band of a component catalyst flow into the VB of another component catalyst, that yields a higher photo catalytic efficiency to the composite material than the individual component.[17, 18] Since the latter approach enhances the both, charge separation efficiency and redox capability of the material, designing and fabrication of a TiO_2-based Z-scheme photocatalyst is of a great interest to scientific community.

Recently, graphite like carbon nitride (g-C_3N_4), as a metal-free and n-type semiconductor, has attracted extensive attentions in the photocatalysis field.[19] The special structural feature of the material, i.e., tris-s-triazine unit, yields high stability under light irradiation with a wide range of working pH 0-14 and benefits to human kind.[20] Although the level of VB in graphitic carbon nitride, having a narrow (2.7 eV) band gap, is not high enough to oxidize water molecule, g-C_3N_4 could be a perfect choice to fabricate herojunction structures by combining with other semiconductors, which yields greater photocatalytic efficiency to the material.[21-24] Recently, there have been several reports on hybrids of g-C_3N_4 with TiO_2.[25-28] A study on photodegradation of RhB using g-C_3N_4–TiO_2 under visible light irradiation[29] demonstrated that there was band–band transfer of VB and CB and a formation of greater quantity of superoxide radicals/ions. However, the Z-scheme principle transfer was reported to be taken place in g-C_3N_4–TiO_2 under UV light irradiation along with a formation of hydroxyl radicals (•OH) to a greater extent.[28, 30]

In the present work, a hybridized and self-doped photoelectrocatalytic material (g-C_3N_4–Ti^{3+}/TiO_2) was prepared by a simple two step process involving heat treatment and in-situ electrochemical reduction doping. The photoelectrocatalytic activity of the material as photo-electrode was examined under visible light irradiation in terms of photodegradation of phenol compound. The characterization of prepared g-C_3N_4–Ti^{3+}/TiO_2 (R-TCNs) was studied in details. The activity of the photo-excited charge carriers (electrons and holes) of the R-TCNs was followed by photoluminescence technique and their separation mechanisms were established.

2. Experimental

2.1. Chemical and material

Titanium sheet with a thickness of 1 mm and a purity of 99.9 % was purchased from Strem Chemicals. The chemicals such as ethylene glycol (EG), ammonia fluoride (NH_4F), sodium sulfate (Na_2SO_4), melamine (Purity 99 %) etc., were purchased from Acros Organics and used as received. The aqueous solution used were prepared using a millipore deionized (DI) water with a resistivity of 18.2 MΩ cm.

2.2. Catalyst preparation

The self-organized TiO_2 nanotube arrays (TNTs) were fabricated on Ti foil substrate (1.5 cm × 2 cm) by anodization method using ethylene glycol (EG) as electrolyte media that contained 0.25 wt % NH_4F and 2 vol % water. The fabrication has been described in detail in our previous studies.[31] The anodization of Ti foil was performed with a two electrode electrochemical system employing platinum mesh as cathode at a constant operating potential of 30 V for a period of 45 min. A two electrode electrochemical system was used for the anodization process employing Ti foil and platinum mesh electrodes as anode and cathode respectively at a constant potential of

Physical Chemistry Chemical Physics Accepted Manuscript

30 V for a period of 45 min. The inter electrode gap was fixed as 4 cm for every electrolysis run. In the post treatment, the anodized sample was washed with deionized water, dried at 70 °C and calcined at 500 °C for 2 h.

The fabrication of g-C_3N_4–TiO_2 (TCNs) composite was carried out as follows: the TNTs was hanged over a ceramic crucible containing melamine of desired quantity and this set-up was put into a muffle furnace operated at 500°C for a period of 2 h. The TCNs with different content of g-C_3N_4 was achieved by placing various quantity of melamine viz. 0.2, 0.3, 0.4 and 0.5 g. The self-doping of Ti^{3+} into g-C_3N_4–TiO_2 arrays was accomplished by an electrochemical reduction method.[31, 32] A conventional three-electrode system was set up by employing the TCNs, Pt sheet and a saturated calomel electrode (SCE) as cathode, anode and reference electrodes, respectively. Initially, the foil of TCNs was subjected to an electrolysis run at cathodic potentials of −1.3 V (*vs* SCE) for 10 min in a 0.1 mol dm^{-3} Na_2SO_4 aqueous solution at room temperature. The thus-prepared R-TCNs were finally cleaned using deionized water and dried at 80 °C.

2.3. Characterization

The morphology study was performed on a field emission scanning electron microscope (FE-SEM, NANOSEM 450, FEI) operating at an accelerating voltage of 30 kV. The phase purity and crystal structure of the obtained samples were examined by X-ray technique using Rigaku Ultima IV XRD (Rigaku Corporation, Japan) equipped with Cu-Kα radiation (40 kV, λ=1.5406 Å), and the 2θ scanning angle range was 20°-80° with a step of 0.05° s^{-1}. The diffuse reflectance spectroscopy (DRS) was obtained from a UV-visible spectrophotometer (UV-2550, Japan) using Ba_2SO_4 as reflectance standard with a spectrum window of 250−800 nm. The X-ray photoelectron spectroscopy (XPS) data were collected by an Axis Ultra instrument

Physical Chemistry Chemical Physics Accepted Manuscript

(Kratos Analytical) under ultra high vacuum (<10^{-8} Torr) using a monochromatic Al Ka X-ray source (*hv* = 1486.6 eV) operating at 150 W.

The electrochemical studies of the prepared samples were carried out by using a electrochemical workstation (CS310, CorrTest, China) with three-electrode configuration employing the photocatalytic material as anode while SCE and Pt mesh were reference and counter electrodes, respectively. The supporting electrolyte used was 0.1 mol dm^{-3} Na_2SO_4 aqueous solution. The light source used was a 11 W incandescent lamp (PHILPS, Netherlands) and the samples were irradiated using the light with an intensity of 3 mW cm^{-2} which was measured by a visible-light radiometer (FZ-A, China).

2.4. Photoelectrocatalytic degradation of phenol under visible light irradiation

Photoelectrocatalytic oxidation experiments were carried out in a glass container having volume capacity of 150 mL with a standard three-electrode configuration electrochemical workstation using synthesized photocatalytic material as photoanode with an exposed area of 1.5 cm × 2 cm. The counter and reference electrodes were a Pt foil and a SCE, respectively. The working volume of the experiments taken was 50 mL aqueous solution that contains phenol (10 mg dm^{-3}) and Na_2SO_4 (0.1 mol dm^{-3}) as target contaminant and supporting electrolyte, respectively. The glass container was placed in a thermostat having continuous water circulation, to regulate the temperature (298 K) and the entire set-up was placed on a magnetic stirrer operated at a constant stirring rate of 650 rpm. Prior to light irradiation, the working solution underwent a stirring treatment in the dark for *ca.* 60 min to establish an adsorption/desorption equilibrium between the organic contaminant and the surface of the samples at ambient air equilibrium condition. The concentration of phenol was measured by high performance liquid chromatography (HPLC) (Shimadzu, Japan)

Physical Chemistry Chemical Physics Accepted Manuscript

equipped with a UV detector and a C_{18} reverse-phase column (4.6 mm i.d. ×150 mm, Agilent, USA). The mobile phase used in the HPLC was water and methanol, with a ratio of 50:50 (v/v). The injection volume of the sample was 20 μL and the flow rate was 0.5 mL min^{-1}. The wavelength of the UV absorbance detector was fixed at 270 nm.

Phenol (10 mg dm^{-3}) dissolved in the water sample collected from East Lake of Wuhan city was subjected to PEC by using R-TCNs as photoelectrode to check its feasibility to a real environmental water sample.

2.5. Analysis of hydroxyl radical

The formation of •OH in the photoelectrocatalytic (PEC) process was detected by photoluminescence (PL) technique using terephthalic acid as a probe molecule. Terephthalic acid reacts with •OH to produce a highly fluorescent product 2-hydroxy terephthalic rapidly and specifically, which reflected as the PL signal at 425 nm excited by 315 nm light.[33] The experimental conditions adopted were similar to the PEC process with an exception of replacing phenol solution by a solution containing terephthalic acid and NaOH in the concentration of 1×10^{-3} mol dm^{-3} and 4×10^{-3} mol dm^{-3}, respectively. PL spectra of generated 2-hydroxyterephthalic acid were measured on a fluorescence spectrophotometer (Jasco FP-6200, Japan).

3. Results and discussion

3.1. Optimization of photoelectrocatalytic activity of R-TCNs

To study the effect of different content of g-C_3N_4 on the PEC performance of TiO_2, melamine were added at different quantities such as 0.2, 0.3, 0.4 and 0.5 g, during the heat treatment. It is important to note that the TNTs material was stable enough and not underwent any destruction or damage during the heat treatment. Fig. 1a shows a comparative transient photocurrent response studies performed between the TNTs and

Physical Chemistry Chemical Physics Accepted Manuscript

TCNs samples by applying alternative on–off visible light illumination cycles at +0.6 V *vs.* SCE. The photocurrent densities of the TCNs samples were shown to be at least 1/2 times more than that of the TNTs, which confirmed the impact of CNs in increasing the PEC performance of TNTs. Moreover, the photocurrent densities of TCNs initially got increased as the quantity of melamine increased from 0.2 g to 0.3 g, followed by a decline trend with a further increase of the quantity up to 0.5 g. In addition, upon an electrochemical reduction treatment, the photocurrent responses of TCNs increased to a greater extent dramatically (as shown in Fig. 1b). The R-TCNs prepared at a 0.3 g addition of melamine quantity showed a maximum photocurrent density of about 110 μA cm^{-2},which was about a four times higher efficiency than that of the TNTs (Fig. 1b).

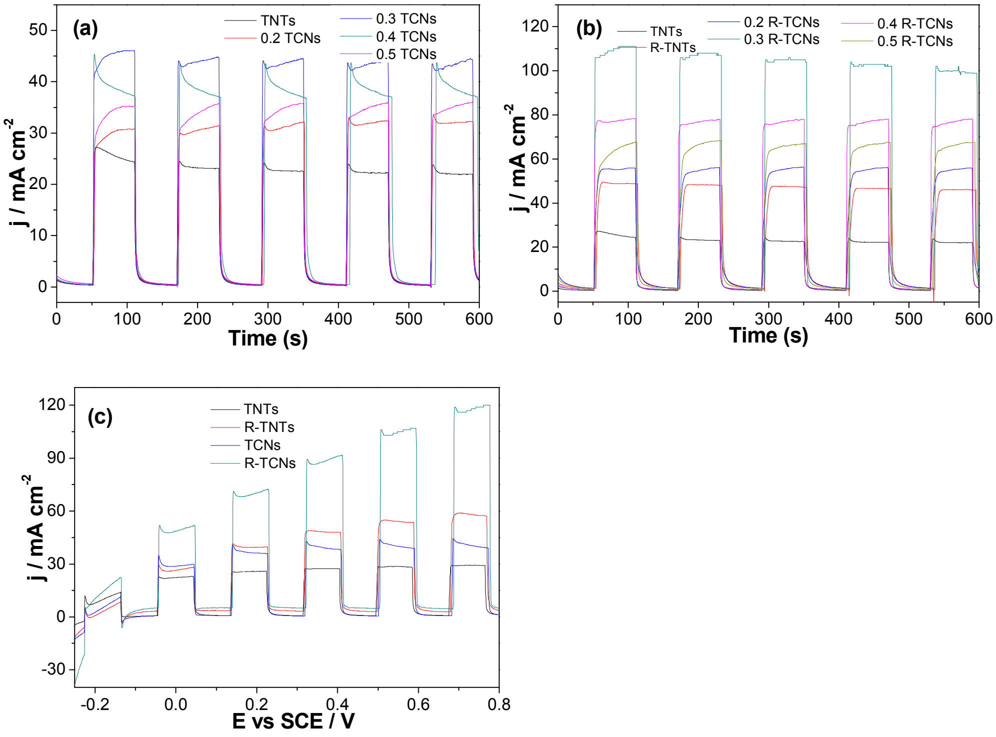

Fig. 1. (a) PEC performance of the composite samples prepared with different content of melamine at +0.6 V vs SCE under visible light irradiation in 0.1 mol dm^{-3} Na_2SO_4 aqueous solution (pH=6.8) and (b) electroreduction at −1.3 V for 10 min, (c)

Physical Chemistry Chemical Physics Accepted Manuscript

LSV curves of TNTs, R-TNTs, TCNs and R-TCNs in 0.1 mol dm^{-3} Na_2SO_4 solution in dark and under visible light irradiation.

Further, to compare the PEC performance of the materials under visible light irradiation, the linear sweeps study was conducted for TNTs, R-TNTs, TCNs and R-TCNs samples processed in the potential range of −0.3 V to + 0.8 V (*vs* SCE) under chopped visible light irradiation (light on-off cycles: 60 s) with a scan rate of 1.5 mV s^{-1}. As seen in Fig. 1c, the photocurrent response of TNTs was found to be enhanced not only by introducing/doping Ti^{3+} but also by compositing the CNs, and this could be easily understood by the observed dramatic increase of photocurrent density due to a cumulative impact of both the treatment.

3.2. Phase structures and morphology

Fig. 2 depicts the XRD patterns of the pure CNs, TNTs, TCNs and R-TCNs samples. As seen, only the anatase phases of TiO_2 were identified in all the TiO_2-based samples. For pure CNs, two main diffraction peaks of 2θ at around 27.4 and 13.6 were observed, corresponding to the (002) and (100) plane diffractions, respectively.[34] For TCNs and R-TCNs, no characteristic diffraction peaks of CNs were observed because of its poor crystallization behavior and less content. Since there was no obvious change in the position, intensity and width of the characteristic diffraction peaks of anatase TiO_2, the presence of CNs was proved to be having no influence on the phase structure of the TNTs.

Physical Chemistry Chemical Physics Accepted Manuscript

Physical Chemistry Chemical Physics Accepted Manuscript

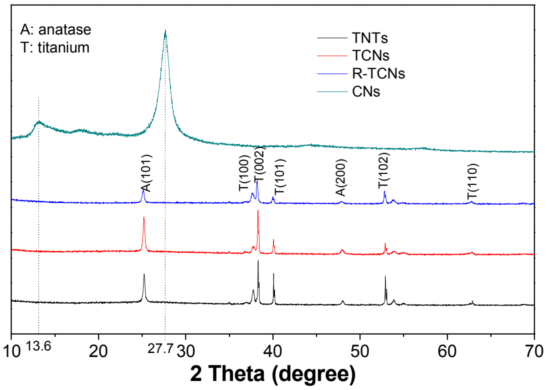

Fig. 2. XRD patterns of the TNTs, TCNs, R-TCNs and pure CNs samples.

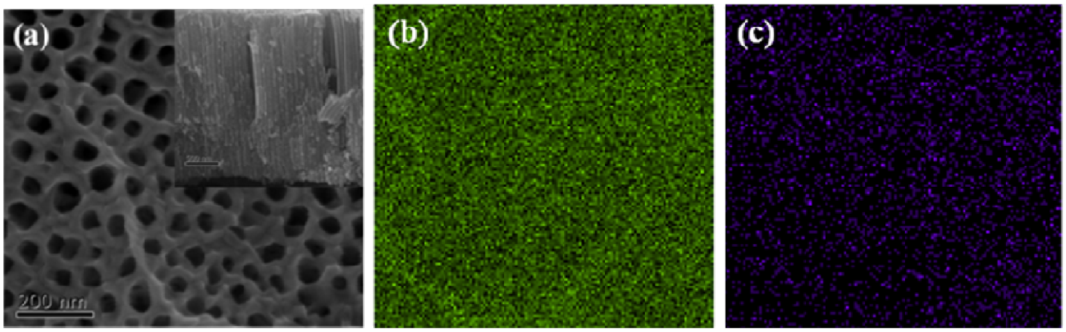

Fig. 3. SEM image of the R-TCNs (the inset shows the cross-sectional image); EDS mapping of Ti element (b) and N element (c) of the R-TCNs.

The microstructure and elements distribution of R-TCNs were studied by using SEM and EDS mapping, respectively. Fig. 3a shows the typical SEM images of R-TCNs prepared by an electrochemical reduction process at −1.3 V for a period of 10 min. The dimensional quality of highly ordered nanotube structure of TNTs was observed to be retained for the R-TCNs suggesting that the hierarchical nanotube structures of the TNTs have been unaltered and not disturbed by both the addition of CNs and the electrochemical reduction treatment. The inset shows a cross-sectional view of the R-TCNs, in which the nanotube with a length of about 3 μm was observed to be vertically well oriented on the Ti substrate. The finding of elements (Ti and N) from the EDS mapping images (Fig. 3b and 3c), proved the co-existence of both titanium dioxide and carbon nitride. The well dispersion of Ti and N was clearly seen in Fig. 3b and Fig. 3c.

FTIR spectra were recorded for CNs, TNTs and R-TCNs composite samples as shown in Fig. 4. The strong bands observed between 1200–1600 cm^{-1} with the characteristic peaks at 1241, 1319, 1403, 1465 and 1573 cm^{-1} could be attributed to typical stretching vibrations of the C–N heterocycle compounds.[35] The peak at 810 cm^{-1} could be attributed to the characteristic breathing mode of triazine units.[36] A broad band observed in the range of 3150–3300 cm^{-1} corresponded to stretching vibration modes of terminal NH groups.[37] Pure TNTs exhibited a characteristic absorption band broadly over 500–700 cm^{-1}.[39] The main characteristic peaks correspond to CNs and TNTs appeared for R-TCNs sample strongly declared the formation of composite between CNs and TNTs in the R-TCNs photocatalyst.

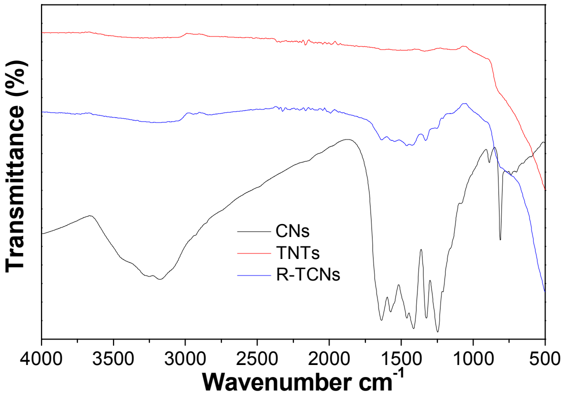

Fig. 4. IR spectra of the TNTs, R-TCNs and CNs samples.

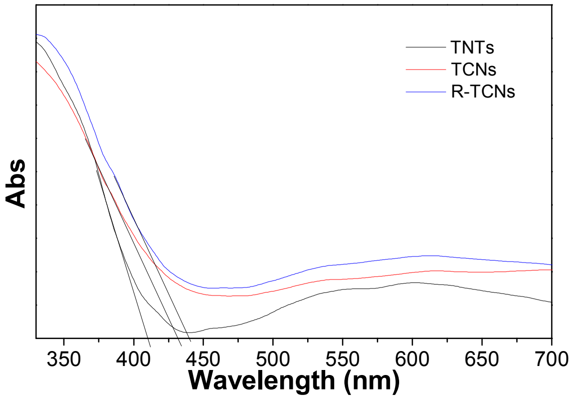

Physical Chemistry Chemical Physics Accepted Manuscript

Fig. 5. UV-vis diffuse reflection spectra of the TNTs, TCNs, R-TCNs and pure CNs samples.

As seen in Fig.5, the optical responses of the photocatalytic film were investigated by UV-vis DRS. A sharp edge of basal absorption for TiO_2 sample was moved up to ~ 410 nm (3.02 eV) and upon the incorporation of CNs, i.e., for TCNs sample, it was extended to 430 nm and distinctly established in visible light region. In the case of TCNs, the bandgap absorption edge was reduced to 2.89 eV caused the absorption of visible-light by CNs.[19] Further, upon electroreduction process of the TCNs sample, i.e., for R-TCNs, the light absorption was extended to still longer wavelength region and the appearance of highest red shift was to a maximum of 445 nm (2.78 eV). These observations clearly indicated that the incorporation of composite material and the self-doping of Ti^{3+} could provide the photocatalyst with a capacity of utilizing the visible light very effectively.

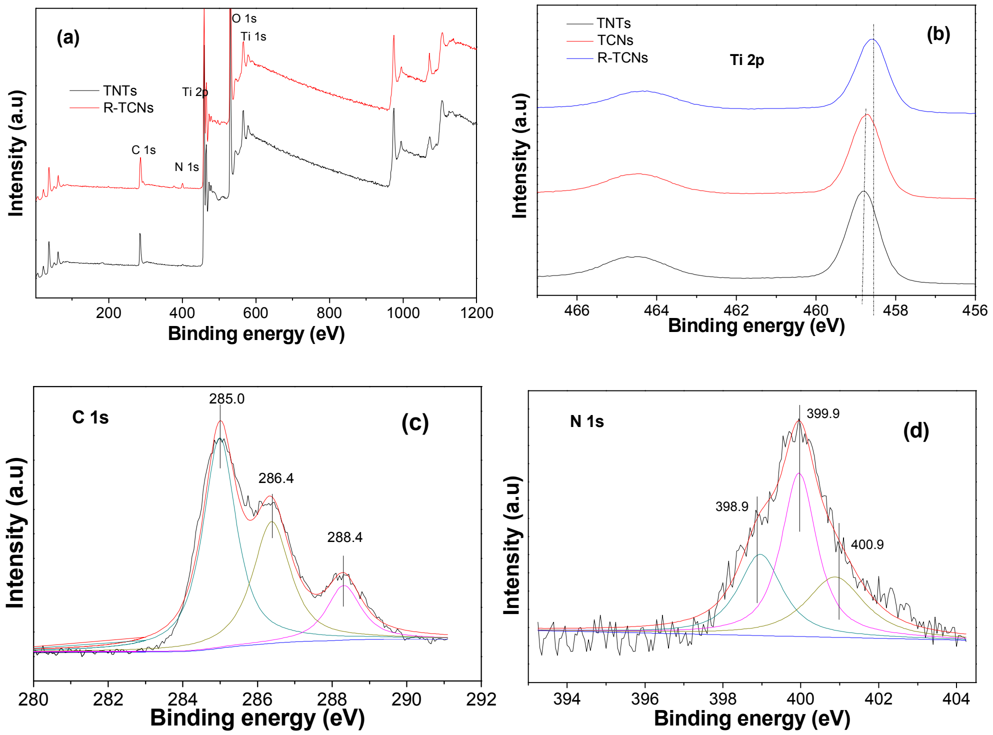

Physical Chemistry Chemical Physics Accepted Manuscript

Fig. 6. XPS survey spectrum (a) of the TNTs and R-TCNs. High resolution XPS spectra of C 1s (b) and N 1s (c) for the R-TCNs, and Ti 2p (d) for the TNTs, TCNs and R-TCNs.

As shown in Fig. 6, the XPS spectrum for TNTs and R-TCNs were recorded to analyze the chemical composition of the surface of the as prepared samples and find out the chemical nature of the elements (Ti, C, and N) presented in the samples. The peaks correspond to Ti, O, C and N were seen in the case of R-TCNs and the same peaks excluding N, were observed for TNTs. Fig. 6b shows the Ti 2p spectra of TNTs, TCNs and R-TCNs samples. The binding energies of Ti $2p_{3/2}$ and Ti $2p_{1/2}$ observed at 458.8 eV and 464.7 eV, respectively, were found to be identical for both TNTs and TCNs samples, which implied that Ti^{4+} species were presented in the form of TiO_2 clusters.[38, 39] However, the binding energies of Ti $2p_{3/2}$ and Ti $2p_{1/2}$ had a lower shift of ~0.3 eV for R-TCNs sample. The lower shift could be due to a electronegative effect of the samples developed by Ti^{3+} doping in the lattices, which actually enhanced a partial electron transformation and in turn an increased electron density on Ti.[31, 32, 40]

As seen in Fig. 6c, high resolution C 1s spectrum was recorded for R-TCNs sample and found to be having three peaks in order. The one located at 285.1 eV was due to C—C and/or adventitious carbon and the following peaks at 286.4 and 288.4 eV could be accounted for the C—N—C and C—$(N)_3$ groups of CNs, respectively.[41] No peak corresponding to chemical interaction between Ti and C (Ti–C) was seen for both TCNs and R-TCNs samples in the XPS (Fig. 6c) studies. It clearly revealed that no chemical interaction took place between CNs and TNTs, i.e. CNs had only been physically coated on the surface of the TiO_2. In addition, the regional spectrum of N 1s for R-TCNs was studied as seen in Fig. 6d. The spectrum could be deconvolved

Physical Chemistry Chemical Physics Accepted Manuscript

Physical Chemistry Chemical Physics Accepted Manuscript

into three peaks viz. 398.9, 399.9, 400.9 eV, which could be accounted for C—N=C, N—(C)$_3$ and —NH$_2$ or =NH of uncondensed terminal amino groups of the material, respectively.[25, 41] It was quite clear from the results that the CNs was more stable and not underwent any reduction during the electrochemical reduction treatment. The results of XPS along with that of SEM, DRS and FTIR studies have been strongly declared that no apparent characteristic Ti–C(N) coordination peaks were observed as the composite material was a simple physical mixture of two separate phases of g-C_3N_4 and TiO_2.

3.3. Photoelectrocatalytic activity of R-TNTs towards the degradation of phenol

Since the phenol compound is known to be a highly toxic, persistent and biorecalcitrant pollutant, and its presence in ground and surface water is considered to be a direct threat to health of humankind, the PEC activity of the prepared samples was evaluated in terms of degradation of phenol with a concentration of 10 mg dm^{-3}. As shown in Fig. 7a, the concentration of phenol was steadily decreased with illumination time during the PEC process using an incandescent light ($\lambda > 420$ nm) at a bias potential of + 0.6 V *vs* SCE. At a reaction period of 7 h, the degradation was only 23.4 % using TNTs electrode, while it was increased up to more than 45% using the sample incorporated by CNs. Importantly, the degradation % was reached to a maximum of 74% using the R-TCNs sample i.e., self-doping of Ti^{3+} into TCNs by electrochemical reduction enhanced the photocatalytic activity of the TiO_2 based composite material to a greater extent. In addition, the concentration of phenol in the water samples from East Lake was also decreased steadily in the PEC process by R-TCNs electrode. As shown in Fig. 7b, the degradation rate was about 60%, which demonstrated that the R-TCNs is a promising nanomaterial to remove phenol in a real environmental water by means of PEC technique.

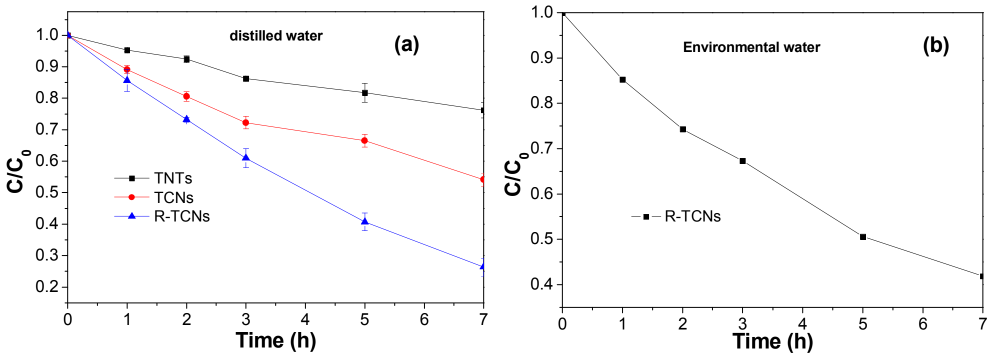

Fig. 7. (a) Comparison of the degradation rate of phenol among the TNTs, TCNs and R-TCNs photoelectrodes in distilled water, and (b) in the environmental water sample (East Lake) by R-TCNs photoelectrodes under visible light irradiation (λ > 420 nm, 3 mW/cm^2, +0.6 V *vs* SCE).

The generation of •OH was quantitatively analyzed by photoluminescence (PL) method with an aim of understanding the mechanism of PEC process and investigating the active species involved in the process. The respective PL signals for CNs, TNTs, TCNs and R-TCNs samples as photoanode recorded at 3 h of PEC process are seen in Fig. 8. It could be easily understood that no •OH was generated during the PEC process using CNs as there was no corresponding PL signal. The absence of •OH radicals in the PEC process of CNs could be well explained by the relationship between the position of the VB edges (E_v) of CNs and the actual formation potential of the OH^-/•OH couple (+1.83 V / +2.7 V) versus NHE. i.e., the photogenerated holes on the surface of the CNs was not strong enough to oxidize the OH^- or H_2O into •OH.[30, 40] On the other hand, the formation of •OH was observed for TNTs, TCNs and R-TCNs photoanode samples, among which, the greater quantity of •OH was found to be produced only from R-TCNs compared to TNTs and TCNs.

Physical Chemistry Chemical Physics Accepted Manuscript

Physical Chemistry Chemical Physics Accepted Manuscript

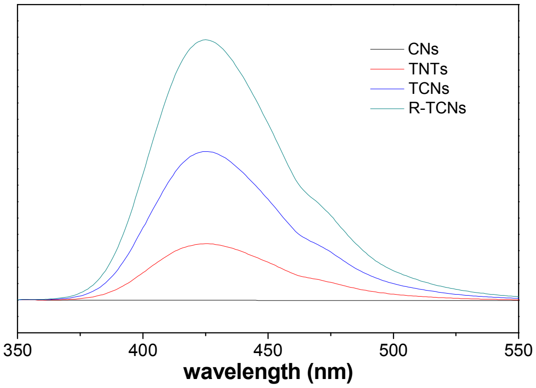

Fig. 8. PL spectra of TNTs, TCNs and R-TCNs in a 1×10^{-3} mol dm^{-3} basic solution of terephthalic acid under visible light irradiation after 3 h of PEC process.

In the case of pristine TiO_2, the position of the photoexcited holes is more positive than the OH^-/•OH couple, thus, the oxidation of OH^-/H_2O to form •OH becomes quite possible. Upon the CNs incorporation, considering the quantity of •OH generated in each case, the formation of Z-scheme $g\text{-}C_3N_4$ –TiO_2 photocatalytic system could possibly be expected. Furthermore, the generation of larger quantity of •OH for an effective degradation of phenol could very well be understood by an efficient space separation between the heterojunction of the composite.

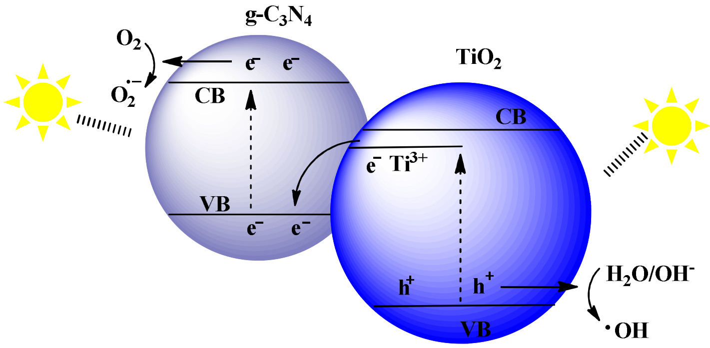

Fig. 9. Schematic illustration for the charge transfer and separation in Z-scheme $g\text{-}C_3N_4\text{–}Ti^{3+}/TiO_2$ photocatalysts under visible light irradiation.

Physical Chemistry Chemical Physics Accepted Manuscript

Our earlier studies on self-doped TNTs photoelectrodes (R-TNTs) have confirmed that the enhancement of the PEC activity of R-TNTs in the visible regions was due to an effective absorption of visible light spectrum and an enhancement in the carrier density as well. The extent of self-doping of Ti^{3+}, which actually existed in the form of $O^{\bullet}_{v}Ti^{3+}$ in the band gap of TiO_2 could enhance the PEC activity of the material in the visible region.[43] Further, the self-doping step could decrease the charge transfer resistance between the solid-electrolyte interface, [31] which resulted in enhanced PEC activity of R-TNTs and greater quantity of •OH generation than that of TNT samples.

Based on the above findings, a possible mechanism for PEC activity of the R-TCNs composite sample was proposed and schematically illustrated in Fig. 10. In the case of TNTs and R-TNTs photoanode, the photo-generated electrons and holes tendded to recombine and only a limited charge carriers took part in the PEC reaction, resulting in relatively lower catalytic activity. Whereas in the case of R-TCNs with an optimized content of CNs, exhibiting Z-scheme g-C_3N_4–Ti^{3+}/TiO_2 PEC activity, the photo-induced holes tended to stay in the VB of TiO_2, while the electrons transferred from the CB of TiO_2 to the VB of g-C_3N_4 and thus, left the higher CB of g-C_3N_4 as the composite one under visible light irradiation. This resulted in an efficient space separation of the photo-induced charge carriers and an enhancement in their oxidation-reduction ability, which the holes in the VB of TiO_2 could react with the water molecules (or surface hydroxyls) adsorbed at the surface of TiO_2 and form more quantity of •OH. Consequently, the phenol molecule got oxidized by the produced •OH and converted into fragmented molecules. The results obtained on the quantitative analysis of •OH strongly suggested the Z-scheme g-C_3N_4–Ti^{3+}/TiO_2 PEC mechanism. Initially the CNs and R-TNTs formed a conventional g-C_3N_4–Ti^{3+}/TiO_2 heterojunction, and hence the photo-induced holes tended to transfer from the VB of

Physical Chemistry Chemical Physics Accepted Manuscript

R-TNTs to the VB of CNs during the PEC process; while the electrons transfer from CB of CNs to CB of R-TNTs，which caused an efficient space separation of the photo-induced charge carriers as well. However, the holes in the VB of CNs not strong enough to reacted with water molecules/surface hydroxyls adsorbed at the surface of CNs and generating no •OH, because the position of VB of CNs was higher than the formation of potential of H_2O/•OH couple. Thus, the PEC activity of the TNTs composite was less than that of the TCNs and R-TCNs samples. From all these findings, it could be concluded that the PEC reaction of R-TCNs followed Z-scheme mechanism.

4. Conclusions

The preparation of TNTs based photocatalytic composite material, Z-scheme g-C_3N_4–Ti^{3+}/TiO_2, was achieved using melamine as precursors, by two step process involving a calcination and in-situ electrochemical reduction doping. The formation of Z-scheme g-C_3N_4–Ti^{3+}/TiO_2 composite photocatalytic material was confirmed by various characterization techniques. The PEC activity of the material was found to be influenced by the incorporated both g-C_3N_4 and Ti^{3+}. At the optimal content of g-C_3N_4, the apparent photocurrent density of the composite TCNs was two times higher than that of the pristine TiO_2 under visible-light illumination. The self-doping of Ti^{3+} into crystal lattice of TiO_2 was found to enhance further the PEC activity of the TCNs. The photocurrent density of R-TCNs photoanode was four times higher than that of the pristine TiO_2, and the corresponding phenol degradation was upto a maximum of 74%. The self-doping of Ti^{3+} promoted the visible light absorption behavior of the composite and enhanced the PEC activity. It was confirmed that the formed photocatalytic composite material was Z-scheme g-C_3N_4–Ti^{3+}/TiO_2 by its efficient space separation of the photo-generated electron–hole. The cumulative impact of both

$g\text{-}C_3N_4$ and Ti^{3+} was responsible for the enhanced PEC activity of $g\text{-}C_3N_4\text{–}Ti^{3+}/TiO_2$ composite material. Conclusively, the present study will provide innovative insights in developing a TiO_2 based photocatalyst ($g\text{-}C_3N_4\text{–}Ti^{3+}/TiO_2$ Z-scheme) with an enhanced PEC activity, by widening the spectral absorption range in to visible region and refraining the recombination of the photogenerated electron–hole charge carriers.

Acknowledgements

This work was supported by the International Science & Technology Cooperation Program of China (No. 2013DFG50150), the National Natural Science Foundation of China (No. 51079056/E090301), and the fundamental research funds for the Central Universities HUST (No. 2014TS094). The authors thank the Analytical and Testing Center of HUST for the use of SEM, XRD, XPS and DRS equipments.

Physical Chemistry Chemical Physics Accepted Manuscript

References:

1 R. Asahi, T. Morikawa, T. Ohwaki, K. Aoki, Y. Taga, *Science*, 2001, **293**, 269.

2 H. Tong, S. Ouyang, Y. Bi, N. Umezawa, M. Oshikiri, J. Ye, *Adv. Mater.*, 2012, **24**, 229.

3 G. Wang, H. Wang, Y. Ling, Y. Tang, X. Yang, R.C. Fitzmorris, C. Wang, J.Z. Zhang, Y. Li, *Nano Lett.*, 2011, **11**, 3026.

4 M. Wang, J. Ioccozia, L. Sun, C. Lin, Z. Lin , *Energy Environ. Sci.*, 2014, **7**, 2182.

5 J. Yu, G. Dai, B. Huang, *J. Phys. Chem. C,* 2009, **113**, 16394.

6 S. George, S. Pokhrel, Z. Ji, B.L. Henderson, T. Xia, L. Li, J.I. Zink, A.E. Nel, L. Mädler, *J. Am. Chem. Soc.*, 2011, **133**, 11270.

7 G. Colon, M. Maicu, M.s. Hidalgo, J. Navio, *Appl. Catal. B-Environ.*, 2006, **67**, 41.

8 T. Ohno, N. Murakami, T. Tsubota, H. Nishimura, *Appl. Catal. A-Gen.,* 2008, **349**, 70,

9 L. Samiolo, M. Valigi, D. Gazzoli, R. Amadelli, *Electrochim. Acta*, 2010, **55**, 7788.

10 Z. Zhang, M.N. Hedhili, H. Zhu, P. Wang, *Phys. Chem. Chem. Phys.,* 2013, **15**, 15637.

11 M. Xing, W. Fang, M. Nasir, Y. Ma, J. Zhang, M. Anpo, *J. Catal.,* 2012, **297**, 236.

12 K. Dai, L. Lu, C. Liang, Q. Liu, G. Zhu, *Appl. Catal. B-Environ.,* 2014, **156**, 331.

13 Y. Takahashi, T. Tatsuma, *Langmuir*, 2005, **21**, 12357.

14 J. Su, L. Guo, N. Bao, C.A. Grimes, *Nano Lett.,* 2011, **11**, 1928.

15 Y.C. Zhang, L. Yao, G. Zhang, D.D. Dionysiou, J. Li, X. Du, *Appl. Catal. B-Environ.,* 2014, **144**, 730.

16 X. Dai, M. Xie, S. Meng, X. Fu, S. Chen, *Appl. Catal. B-Environ.,* 2014, **158**, 382.

Physical Chemistry Chemical Physics Accepted Manuscript

17 T. Arai, M. Yanagida, Y. Konishi, Y. Iwasaki, H. Sugihara, K. Sayama, *J. Phys. Chem. C,* 2007, **111**, 7574.

18 Y. Yang, W. Guo, Y. Guo, Y. Zhao, X. Yuan, Y. Guo, *J. Hazard. Mater.,* 2014, **271**, 150.

19 X. Wang, K. Maeda, A. Thomas, K. Takanabe, G. Xin, J.M. Carlsson, K. Domen, M. Antonietti, *Nature Mater.,* 2008, **8**, 76-80.

20 G. Dong, Y. Zhang, Q. Pan, J. Qiu, *J. Photochem. Photobio. C: Photochem. Rev.,* 2014, **20**, 33.

21 Z. Jin, N. Murakami, T. Tsubota, T. Ohno, *Appl. Catal. B-Environ.,* 2014, **150**, 479.

22 Y. Zang, L. Li, X. Li, R. Lin, G. Li, *Chem. Engin. J.,* 2014, **246**, 277.

23 C. Chang, L. Zhu, S. Wang, X. Chu, L. Yue, *ACS Appl. Mater. Interfaces,* **6**, 2014, 5083.

24 J. Chen, S. Shen, P. Guo, M. Wang, P. Wu, X. Wang, L. Guo, Appl. Catal. B-Environ., **152**, 2014, 335.

25 F. Chang, J. Zhang, Y. Xie, J. Chen, C. Li, J. Wang, J. Luo, B. Deng, X. Hu, *Appl. Surf. Sci.,* 2014, **311**, 574.

26 S. Zhou, Y. Liu, J. Li, Y. Wang, G. Jiang, Z. Zhao, D. Wang, A. Duan, J. Liu, Y. Wei, *Appl. Catal. B-Environ.,* 2014, **158**, 20.

27 Z. Tong, D. Yang, T. Xiao, Y. Tian, Z. Jiang, *Chem. Eng. J.,* 260 (2015) 117-125.

28 Q. Sun, K. Lv, Z. Zhang, M. Li, B. Li, *Appl. Catal. B-Environ.,* 2015, **164,** 420.

29 N. Boonprakob, N. Wetchakun, S. Phanichphant, D. Waxler, P. Sherrell, A. Nattestad, J. Chen, B. *J. Colloid. Interf. Sci.,* 2014, **417**, 402.

30 J. Yu, S. Wang, J. Low, W. Xiao, *Phys. Chem. Chem. Phys.,* 2013, **15**, 16883.

Physical Chemistry Chemical Physics Accepted Manuscript

31 W. Liao, J. Yang, H. Zhou, M. Murugananthan, Y. Zhang, *Electrochim. Acta,* 2014, **136**, 310.

32 H. Zhou, Y. Zhang, *J. Phys. Chem. C,* 2014, **11**, 5626.

33 W. Liao, Y. Zhang, M. Zhang, M. Murugananthan, S. Yoshihara, *Chem. Eng. J.,* 2013, **231**, 455.

34 A. Thomas, A. Fischer, F. Goettmann, M. Antonietti, J.-O. Müller, R. Schlögl, J.M. Carlsson, *J. Mater. Chem.,* 2008, **18**, 4893.

35 S. Yan, Z. Li, Z. Zou, *Langmuir,* 2009, **25**, 10397.

36 Y. Zhang, A. Thomas, M. Antonietti, X. Wang, *J. Am. Chem. Soc.,* 2008, **131**, 50.

37 X. Wang, X. Chen, A. Thomas, X. Fu, M. Antonietti, *Adv. Mater.,* 2009, **21**, 1609.

38 X. Lu, G. Wang, T. Zhai, M. Yu, J. Gan, Y. Tong, Y. Li, *Nano Lett.,* 2012, **12**,1690.

39 W.-D. Zhu, C.-W. Wang, J.-B. Chen, Y. Li, J. Wang, *Appl. Surf. Sci.,* 2014, **301**, 525.

40 M. Xing, W. Fang, M. Nasir, Y. Ma, J. Zhang, M. Anpo, *J. Catal.,* 2013, **297,** 236.

41 S. Yan, Z. Li, Z. Zou, *Langmuir,* 2010, **26**, 3894.

42 S. Chen, Y. Hu, S. Meng, X. Fu, *Appl. Catal. B-Environ.,* 2014, **150**, 564.

43 M. Xing, J. Zhang, F. Chen, B. Tian, *Chem. Commu.,* 2011, **47**, 4947.

Physical Chemistry Chemical Physics Accepted Manuscript